Available online at www.sciencedirect.com
ScienceDirect
Journal of Molecular Catalysis A: Chemical 258 (2006) 15–21
JOURNAL OF MOLECULAR CATALYSIS A: CHEMICAL
www.elsevier.com/locate/molcata

Effect of acidity and porosity changes of dealuminated mordenites on *n*-hexane isomerization

N. Viswanadham *, Lalji Dixit, J.K. Gupta, M.O. Garg

Catalysis and Conversion Process Division, Indian Institute of Petroleum, Dehradun-248005, India

Received 14 December 2005; received in revised form 25 April 2006; accepted 26 April 2006
Available online 15 June 2006

Abstract

A series of dealuminated mordenite samples was prepared and tested for their activity in *n*-hexane hydroisomerization reaction. The samples were thoroughly characterized by XRD, microcalorimetry, and adsorption measurement to obtain surface area, pore volume and pore size distribution. Both strong acidity ($\Delta H_{NH_3} > 100\,kJ/mol$) and micropore volume (0–20 Å) of the mordenite were increased during the initial stage of dealumination. Further dealumination caused very little or negligible improvement in the catalytic properties. Among the various catalysts prepared, the catalyst dealuminated by steaming at 673 K, followed by acid leaching with 2N HNO_3 (S2-HM) exhibited highest amount of strong acidity and isomer yields in *n*-hexane conversion. The selectivity to di-branched isomers was continuously increased with dealumination.

Keywords: Mordenite; Steaming; Dealumination; Strong acidity; Micropore; Isomer yield

1. Introduction

Enhancement of catalytic activity of zeolites by mild dealumination is a well-known phenomenon [1]. For Y zeolite it is due to the increase in acid strength of remaining aluminum sites after removal of nearest aluminum neighbors in zeolite by dealumination [2]. For ZSM-5, it is mainly due to the partial hydrolysis of framework aluminum and the high turnover frequency of the acid sites associated with the EFAL [3,4]. The dealumination of mordenite was also observed to improve the catalytic activity in hydroisomerization of light alkanes [5,6]. But, there is a difference of opinion regarding the factors responsible for such enhancement.

The proton form of mordenite in combination with a noble metal, Pt can effectively catalyze the reactions such as skeletal isomerization, hydrogenation and dehydrogenation for the production of environment-friendly, high-octane isomerate [7,8]. In general mordenite catalysts undergo rapid deactivation because of their uni-dimensional pore system with a small side pockets that are generally not accessible to reactant molecules. However, by adopting some post synthesis modification methods such as framework dealumination, mordenite has been successfully operating in industrial processes viz. DOW's process for cumene production [9–11] and Shell's process for hydroisomerization of linear alkanes [12,13].

The beneficial effect of framework dealumination of mordenite was mostly ascribed to the improvement in porosity of the mordenite and increased diffusion of the reaction molecules [14–17]. Nagano et al. have studied the microporous structure of dealuminated mordenite by ^{1}H and ^{129}Xe NMR using methane and xenon probe molecules. They observed increase in pores of both the main channels and the side pockets of dealuminated mordenite, though the increase is significant in case of side pockets [18]. van Donk et al. have reported the formation of mesopores in acid-leached mordenite and their influence on increased uptake of *n*-hexane and its hydroisomerization activity [19]. Meyers et al. observed the increase in pore volume of the mordenite after acid treatment [20]. van Tromp et al. observed the accessibility of side pockets of mordenite to isopropylamine after acid leaching but not before acid leaching [21]. Goovaerts et al. reported that the dealumination in mordenite led to increased microporosity as it occurred preferentially at lattice defects, thus opening the main channels, or generate secondary micropores by connecting side pockets of adjacent channels [22]. Recent studies of Nesterenko et al. also indicated increased

* Corresponding author.
E-mail addresses: nvish@iip.res.in, nviswanadham@india.com (N. Viswanadham).

1381-1169/$ – see front matter © 2006 Elsevier B.V. All rights reserved.
doi:10.1016/j.molcata.2006.04.067

accessibility of acid sites for gas phase adsorption of bulky base molecules after dealumination of mordenite [23].

Acidity is another important factor that varies with the framework dealumination of zeolites. Dealumination causes decrease in the total number of acid sties, but the strength of remaining sites may increase as a result of the decrease in the number of atoms sharing the charge (media effect). Such acid sites are observed to improve the hydroisomerization activity of light alkanes [14]. As aluminum in the zeolite framework is the source of acidity, an optimum value of the framework Si/Al ratio is needed to achieve the maximum catalytic activity [24–26]. For example, Koriada et al. have shown that after acid washing both the activity and selectivity for pentane isomerization reached a peak at a Si/Al ratio of 8.5 [27]. However, the studies of Almanza and Narbeshuber and van Bokhoven et al. proposed the increase in surface coverage of alkane as the reason for enhanced activity after steam dealumination [28,29].

The aim of the present study is to investigate the structural changes occurring in mordenite at different levels of dealumination achieved by steaming and acid leaching treatments and their influence on conversion and product selectivity in *n*-hexane hydroisomerization.

2. Experimental

2.1. Catalyst preparation

Commercial mordenite of Si/Al (atomic ratio) = 16–18, in a powder form, supplied by Sued-Chemie India Ltd. was used as the parent sample (HM). Steaming and acid treatment were used for the framework dealumination. Steaming was carried out in a fixed bed shallow reactor at 573, 673, 773 and 883 K temperatures with a water pressure of 500 mbar. All the steamed samples were treated with 2N nitric acid (99.9% pure, Merck) in a round-bottomed flask in 1:3 zeolite: acid volume ratios under refluxing at 373 K for 1 h. The mixture was filtered, and the solid was washed with distilled water and allowed to dry. Extrudates of the samples were prepared by mixing mordenite and alumina binders in a 60:40 ratio, followed by dropwise addition of 3 vol.% glacial acetic acid and allowing them to peptize for 2 h. The resultant paste was extruded to 1 mm diameter extrudates that were dried at room temperature overnight, followed by heating at 100 °C for 10 h. All the extrudates were calcined at 500 °C for 4 h, before use for metal impregnation. The incipient wetness method was used for the loading of Pt salt. The samples prepared using parent mordenite and four samples steamed at 573, 673, 773 and 873 K were named HM, S1-HM, S2-HM, S3-HM and S4-HM, respectively. All the samples were reduced in presence of hydrogen prior to isomerization reaction.

2.2. Physico-chemical characteristics

X-ray diffraction pattern for all the samples were recorded with a powder X-ray diffractometer model Rigaku Dmax-III B. The measurements were conducted in a continuous $\theta/2\theta$ scan refraction mode using Cu Kα radiation. Surface area and pore size distribution of samples were determined volumetrically by physisorption of nitrogen at liquid temperature (77 K) using an ASAP-2010 Micromeritics (USA) instrument. N_2 adsorption–desorption isotherms were obtained at 77 K. Acidity was characterized by a Setaram C-80 heat flow microcalorimeter which was attached to a volumetric adsorption unit for probe delivery. About 0.1 g of catalyst was outgassed at 723 K under vacuum. The microcalorimetric measurement of ammonia adsorption was carried out at 448 K. Differential heat of ammonia adsorption was determined by introducing small quantities of ammonia on to the outgassed sample, till the neutralization of all acid sites occurred on the catalyst surface. The heat of adsorption evolved for each dose was calculated from the resulting thermograms and the amount of ammonia adsorbed was calculated from the pressure change.

2.3. Catalyst evaluation studies

The catalyst evaluation was conducted in a fixed bed down flow microreactor by loading 5 cm^3 of catalyst. The catalyst is reduced in situ at 773 K, 5 bar, and 12 $l\,h^{-1}$ hydrogen flow, for 4 h. Hydroisomerization reaction was performed at 523 K, 10 bar, 2.3 h^{-1} WHSV, and a H_2/*n*-hexane molar ratio of 2. The product was analyzed by a gas chromatograph and the conversion and selectivities of the products were calculated based on the carbon number of the components as defined by the formulae given below

$$\text{selectivity (C\%)} = \frac{\text{product}}{\text{consumed } n\text{-hexane}} \times 100,$$

$$\text{yield (\%)} = \text{conversion} \times \text{selectivity}$$

3. Results and discussion

3.1. Physico-chemical properties of catalysts

X-ray diffraction patterns of the parent and four acid-leached mordenite samples are given in Fig. 1. All the samples exhibited similar X-ray diffraction patterns indicating the structural integrity of the mordenite even after the dealumination. How-

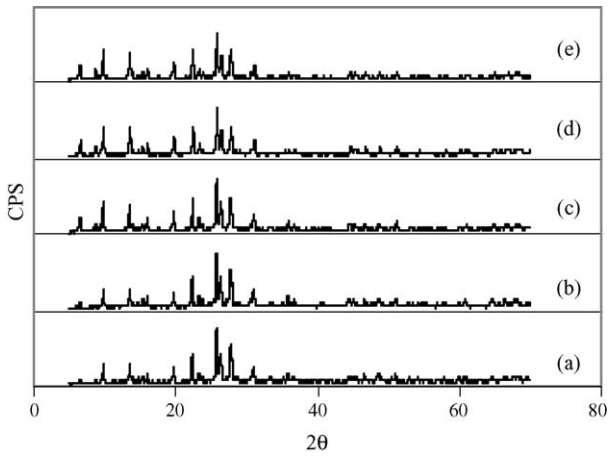

Fig. 1. X-ray diffraction patterns of the mordenite samples (a) HM, (b) S1-HM, (c) S2-HM, (d) S3-HM, and (e) S4-HM.

Table 1
Physico-chemical properties of the mordenite samples

Sample	Si/Al (bulk) XRF	BET area (m^2/g)	Pore volume (cm^3/g)		Crystal-linity (%)	Micro calorimetry acidity (mmol/g. catal)[a]			
			Total	Micro (0–20 Å)		Total	Strong	Medium	Weak
HM	18	283	0.256	0.1063	100	1.48	0.36	0.57	0.55
S1-HM	20	328.9	0.249	0.1249	98	1.40	0.38	0.50	0.52
S2-HM	32	360	0.252	0.1418	95	1.20	0.42	0.38	0.40
S3-HM	39	347	0.254	0.1468	90	1.04	0.40	0.31	0.33
S4-HM	50	302	0.247	0.1469	84	0.86	0.34	0.24	0.28

[a]Total acidity = 160–70 kJ/mol, strong acidity = >100 kJ/mol, medium acidity = 100-75 kJ/mol and weak acidity = <75 kJ/mol.

ever, a gradual increase in the intensities of low angle X-ray diffraction peaks (2θ = 0–20) was observed with increasing severity of acid leaching, i.e., from HM to S4-HM. As the framework aluminum is known to influence hydrophilicity and the intensity of low angle peaks of zeolites, the increased intensity of low angle peaks of dealuminated mordenite of the present study can be ascribed to the increased hydrophobic nature of the mordenite by steaming [30]. The crystallinity was decreased to a small extent of 98% and 95% under mild dealumination conditions (S1-HM and S2-HM), whereas the lowest crystallinity of 84% was observed for the highly dealuminated sample S4-HM. Si/Al ratios calculated from X-ray fluorescence spectroscopy of the samples indicated the occurrence of framework dealumination, where the ratios increased from 18 in the parent mordenite HM to 50 in the S4-HM sample.

The total pore volume of the mordenite did not change but the micropore volume (0–20 Å) was increased with dealumination. A careful analysis of the data indicated three distinguished stages in the increase in the micropore volume, namely, (1) a significant increase from 0.1063 cm^3/g of HM to 0.1418 cm^3/g of S2-HM, (2) a moderate increase to 0.1468 cm^3/g in S3-HM, and (3) a negligible increase to 0.1469 cm^3/g in S4-HM. The micropore volume was increased upon mild dealumination conditions (HM to S3-HM) and leveled off upon severe dealumination conditions (S3-HM to S4-HM). The increase in the micropore volume of the samples after acid leaching may be due to the opening of the side pockets of the mordenite and the formation of micropores larger than mordenite pore channels upon dealumination. As was reported earlier, most of the side pockets of the mordenite are generally closed in as-synthesized samples [21]. Upon acid leaching, dealumination occurs preferentially in such pockets and facilitates the opening of the side pockets. The significant increase in the micropore volume observed up to S2-HM (Si/Al = 32) indicates the side pocket opening. Further dealumination caused an only minimal increase in the micropore volume, which reached a saturation level at S3-HM and S4-HM. The experimental evidence for micropore opening of mordenite was indeed observed and discussed earlier [31].

The increase in the micropore volume of the samples was also reflected in the increased surface area of the samples after dealumination. The surface area of the mordenite was increased from 283 m^2/g HM to 360 m^2/g (S2-HM) and then decreased to 347 m^2/g (S3-HM) and 302 m^2/g (S4-HM). Surface areas of all the dealuminated samples were much higher than that of the parent mordenite. These results support the improvement in mordenite porosity after dealumination.

Acidity of mordenite samples were measured from heats of adsorption of ammonia by microcalorimetry. The amount of ammonia adsorbed per gram of catalyst was considered as the total acidity. The acidity is arbitrarily classified into (a) strong acidity (heat of adsorption > 100 kJ/mol, (b) medium acidity (heat of adsorption from 100 to 75 kJ/mol) and (c) weak acidity (heat of adsorption <75 kJ/mol). As indicated in Table 1, the total acidity of the samples decreased from 1.48 mmol/g in HM to 0.86 mmol/g in S4-HM. The medium and weak acid sites also followed a similar trend; they continuously decreased with dealumination from 0.57 to 0.24 mmol/g and 0.55 to 0.28 mmol/g, respectively. However, the strong acidity did not follow the same trend, but was increased from 0.36 mmol/g in HM to 0.42 mmol/g in S3-HM. Further dealumination to S4-HM resulted in its decrease to 0.32 mmol/g (S4-HM). Increased strong acidity of the mordenite upon initial dealumination can be explained by the increased accessibility of strong acid sites facilitated by the opening of side pockets. Further dealumination could cause removal of framework aluminum species representing the strong acidity. In the present study, the dealumination conditions adopted in the sample S3-HM seem to be suitable for achieving the strong acidity.

3.2. Enhancement in n-hexane isomerization of dealuminated mordenites

The *n*-hexane conversion and composition of the product obtained over various mordenite catalysts have been summarized in Table 2. The *n*-hexane conversion was increased upon initial dealumination, i.e., from 20 wt.% in S1-HM to 43.1 wt.% in S2-HM. Further dealumination caused a decrease in the conversion, which was as low as 31% in S4-HM. The order of *n*-hexane conversion was S2-HM > S3-HM > S4-HM > S1-HM > HM. Isomer yields, the product of *n*-hexane conversion and isomer selectivity, were considered to identify the best catalyst formulation. As can be seen from Fig. 2, the isomer yield passed through a maximum of 41.9 wt.% for S2-HM catalyst. For this catalyst, the *n*-hexane conversion and selectivity were 43.1 wt.% and 97.2%, respectively. Based on these results, S2-HM can be considered as the best catalyst among the five catalysts listed in Table 2.

Table 2
Performance of catalysts in *n*-hexane hydroisomerization

Catalyst	HM	S1-HM	S2-HM	S3-HM	S4-HM
Conversion (wt.%)	20.0	29.5	43.1	36.9	31.0
Selectivity (%)					
Cracking products	0.1	1.1	2.2	2.8	2.6
Methane	0.0	0.0	0.0	0.0	0.0
Ethane	0.0	0.1	0.1	0.2	0.2
Propane	0.05	0.6	1.1	1.5	1.4
Butane	0.05	0.3	0.8	1.0	0.9
Pentane	0.0	0.1	0.2	0.1	0.1
Iso-hexane products	99.0	98.8	97.2	96.5	96.9
2-Methyl pentane	48.6	45.2	43.5	43.2	43.0
3-Methyl pentane	28.5	26.8	26.1	25.4	25.6
2,2-Dimethyl butane	11.5	12.8	13.9	14.0	14.0
2,3-Dimethyl butane	10.4	13.0	13.7	13.9	14.3
Others	0.0	0.1	0.6	0.7	0.5

Reaction conditions: temperature = 523 K, WHSV = 2.3 h^{-1}, and feed = *n*-hexane. Pressure = 10 bar, H_2: HC molar ratio = 2:1.

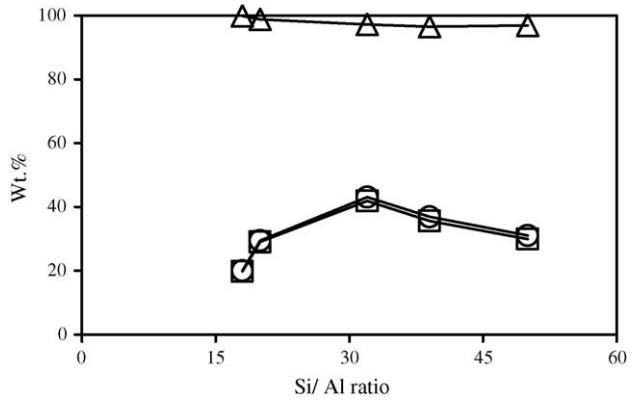

Fig. 2. Effect of dealumination on *n*-hexane isomerization (◯) conversion, (□) isomers yield, and (△) isomers selectivity.

3.3. Performance of S2-HM

The effect of reaction temperature on the conversion and isomer selectivity of S2-HM catalyst can be seen in Fig. 3. The

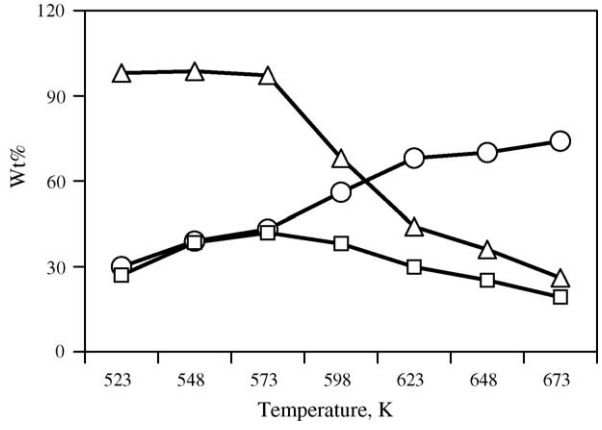

Fig. 3. Effect of reaction temperature (◯) conversion, (□) yield, and (△) isomer selectivity.

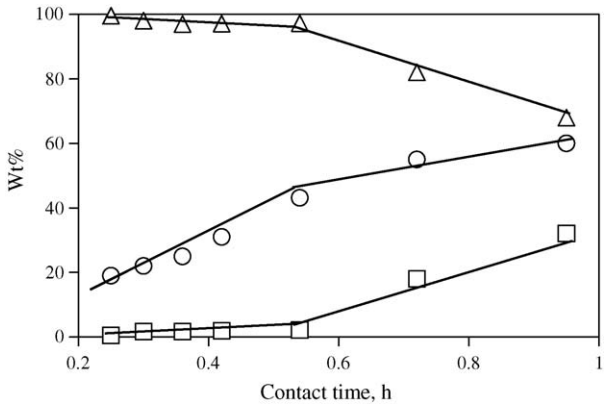

Fig. 4. Effect of contact time: (◯) conversion, (□) cracking selectivity, and (△) isomers selectivity.

conversion was increased significantly from 30 wt.% at 523 K to 70 wt.% at 673 K. Above 673 K, the increase in conversion was minimal (74 wt.%). The *iso*-hexane selectivity was not affected up to 573 K, but was decreased above 573 K (98% at 573 K to 30% in S4-HM). The isomer yield was increased up to 573 K and then decreased above this temperature. The highest isomer yield of 41.9 wt.% was observed at 573 K. The observed trends in isomerization with increasing reaction temperature can be explained by the occurrence of two phenomena, namely, (1) increase in *n*-hexane conversion with reaction temperature (activity factor) and (2) decrease in formation of *iso*-hexane due to the thermodynamic limitations (as the equilibrium favors formation of isomers at lower reaction temperature). With an increase in reaction temperature, the balance between the two oppositely working phenomena might influence the conversion and selectivity, where the optimum reaction temperature was 573 K.

Effect of contact time of the reactant on the conversion and selectivity of isomers over S2-HM at 573 K can be seen in Fig. 4. The conversion increased significantly from 19 wt.% (0.25 h) to 60 wt.% (0.95 h). However, the isomer selectivity was slightly decreased from 99.5% (0.25 h) to 94% (0.54 h) with contact time. Above the contact time of 0.54 h, the isomer selectivity was further declined to as low as 68% at the contact time of 0.95 h. On the other hand, the selectivity to cracking products (C_1–C_5 paraffins) exhibited a just reverse trend to the isomer selectivity. In other words, the isomer selectivity and cracking selectivity followed opposite trends indicating the loss in the isomer selectivity at higher contact time was indeed due to the increase in the cracking selectivity.

3.4. Factors responsible for the enhanced isomerization activity of S2-HM catalyst

Increase in isomer yields on the dealuminated mordenite is in agreement with the literature reports [21,27–29]. In the present study, dealumination caused two major changes in catalytic properties, namely, acidity and microporosity. With acid dealumination, both strong acidity and micropore volume were increased up to the sample S2-HM. Since, the sample S2-HM exhibited the highest isomer yield, either one or the combina-

tion of both acidity and microporosity are responsible for the increase in isomerization activity of dealuminated mordenites.

Evaluation of acidity data indicated the continuous decrease in total acidity with dealumination. Since isomer yields were increased after dealumination, all the acid sites measured by microcalorimetry should not be responsible for the enhanced isomerization. However, the ammonia adsorbed on strong acid sites (heat of adsorption > 100 kJ/mol) attained a maximum upon mild dealumination (S2-HM). Both strong acidity and isomer yields were decreased by further dealumination in samples S3-HM and S4-HM. In spite of the higher micropore volume, the samples S3-HM and S4-HM could not yield more isomers than S2-HM. Hence, the isomer yields of mordenite samples seem to depend on the strong acidity rather than on the micropore volume.

However, the microporosity was also observed to influence the isomer yields. In spite of lower strong acidity, the S4-HM sample having higher micropore volume exhibited higher isomer yield (30 wt.%) than HM (19.8 wt.%). This observation suggested that microporosity is also playing a role in enhanced isomerization of dealuminated mordenites. This aspect can be further analyzed from pore volume data. Pore size distribution of the samples indicated the formation of micropores after the dealumination and the amount of such pores was increased with dealumination. Though the increase was maximum between S1-HM and S2-HM, there was a continuous increase in micropore volume with dealumination. The isomer yield did not increase continuously but was passing through a maximum at S2-HM. This clearly indicates that the microporosity is not the only factor responsible for increased isomerization activity. This aspect can also be analyzed by comparing microporosity and isomer yield data of three dealuminated samples; S2-HM, S3-HM and S4-HM. If the micropore volume alone was responsible for the enhanced isomerization, all the three samples exhibiting comparable micropore volume should have exhibited similar isomer yields. But the isomer yield was decreased from S2-HM to S3-HM and S4-HM.

Overall, the results indicated that both strong acidity and microporosity are responsible for increased isomer yields, though the influence of one factor dominates the other at different dealumination levels. This can be visualized from Fig. 5, where the isomer yields of all the samples are plotted against the catalytic properties. As can be seen in Fig. 5(A), the isomer yields increased with strong acidity from point "a" to point "d", whereas point "e" corresponding to catalyst S4-HM does not fall on the line but exhibited higher isomer yields. This can be due to the higher microporosity of the S4-HM sample. The role of micropores given in Fig. 5(B) also indicated the increase of isomer yield with increasing microporosity from point "a" to point "c", but there is a reverse trend in isomer yields at points "d" and "e" corresponding to catalysts S3-HM and S4-HM. This may be due to the decrease in strong acidity in these samples. Overall, the trends in Fig. 5(A) and (B) indicate that neither strong acidity nor microporosity could justify the increased isomer yields of dealuminated mordenite. However, a continuous increase in isomer yields (point "a" to point "e" of Fig. 5(C)) was observed with the product of strong acidity and micropore volume indicating the combined influence of strong acidity and micropore volume.

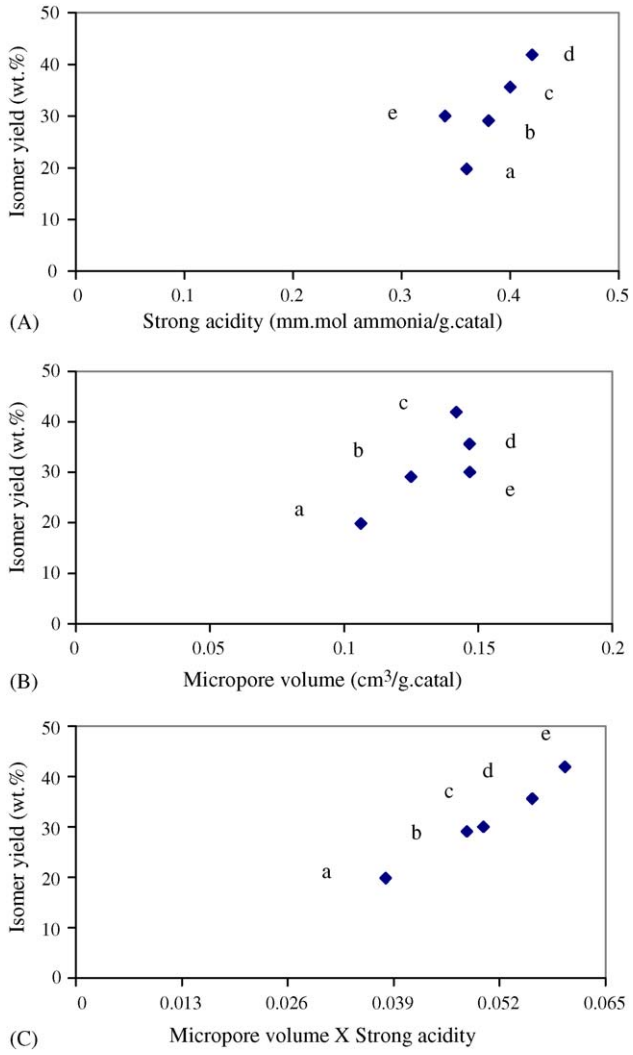

Fig. 5. Factors influencing isomer yields (a) HM, (b) S1-HM, (c) S2-HM, (d) S3-HM, and (e) S4-HM.

Now the question arises about the possible mechanism of dealumination that is effectively altering the strong acidity as well as microporosity. Our earlier studies on porosity measurements indicated the opening of mordenite side pockets upon dealumination [31]. Such phenomenon can improve microporosity as well as the accessibility of strong acid sites present in the side pockets. Improved accessibility of acid sites in dealuminated mordenite was indeed reported by several researchers [18,19,22]. Recent studies of Bucko et al. also indicated the presence of strong acid sites in the side pockets of the mordenite [32]. All these results suggest that the increased isomer yields up to S2-HM can be due to the increased accessibility of strong acid sties in the side pockets of the mordenite facilitated by the opening of the side pockets by dealumination. The decrease in isomer yields above S2-HM can also be understood by the same phenomenon. Under mild dealumination conditions, the increased accessibility of acid sites in side pockets leads to an active catalyst. There is no further increase in acidity by the complete accessibility of all the acid sites to the reactants. Further progression of dealumination can cause removal

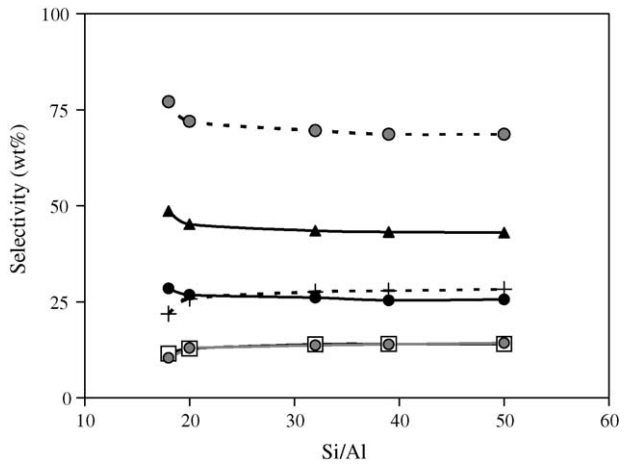

Fig. 6. Effect of dealumination on isomer selectivity. (+) Di-branched, (●) mono-branched, (□) 22 DMC_4, (▲) $2MC_5$ (●) $3MC_5$, and (●) 23 DMC_4.

of aluminum responsible for strong acidity and isomerization activity of the mordenite. Though the increase in microporosity and strong acidity are seemingly different factors, they are commonly related with the single phenomenon of "opening of side pockets" that is responsible for the improved hydroisomerization of *n*-hexane in the present study.

3.5. Selectivity to mono and di-branched isomers

The changes in selectivity to the four isomers of *n*-hexane with increasing dealumination can be seen in Fig. 6. The selectivities to 2-methylpentane and 3-methylpentane were decreased and those to 2,2-dimethylbutane and 2,3-dimethylbutane were increased from HM to S4-HM. In order to see the aspects of the bulkiness of the molecules, the four isomers of *n*-hexane were classified into two groups, namely, mono-branched isomers (2-methylpentane and 3-methylpentane), and di-branched isomers (2,2-dimethylbutane and, 2,3-dimethylbutane). As can be seen in Fig. 6, the selectivity to mono-branched isomers was decreased whereas that to the di-branched was increased with dealumination. The selectivity to di-branched products reached a maximum for the S3-HM sample that also has maximum micropores, indicating the role of micropores in the formation of bulky products.

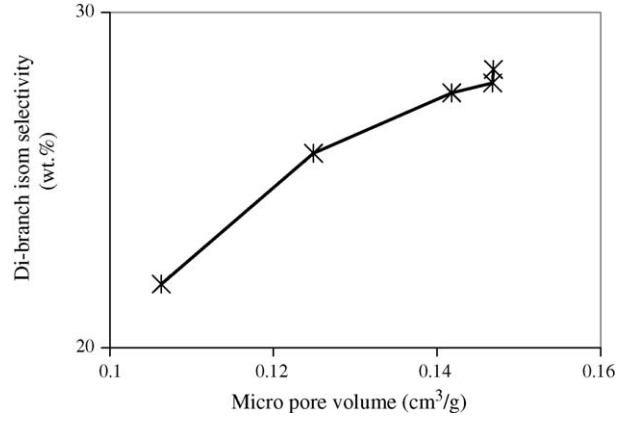

Fig. 7. Effect of micropore volume on di-branching isomers selectivity.

Increased accessibility of the side pockets and the inter connectivity of the pore channels (mesopores and micropores) reported by earlier workers also suggest the possibility of increase in diffusion of bulky di-branched isomers in the pores of dealuminated mordenite [18–21]. This dependence of di-branched products on pore volume can be seen in Fig. 7, where the selectivity to di-branched products increased continuously with the micropore volume. This clearly indicates, that the formation of bulky isomers was facilitated due to the increase in the micropore volume of the dealuminated mordenites.

4. Conclusions

Framework dealumination of mordenite caused two changes in properties, namely, microporosity and the strong acidity. These changes are possibly due to the opening of side pockets that can cause increase in micropore volume and increase in accessibility to strong acid sites. The mildly dealuminated sample S2-HM exhibited the best isomer yields due to the optimum acidity. Severe dealumination could give a slight increase in micropore volume, but caused a decrease in strong acidity. The isomer yields of the samples do not depend completely on strong acidity or on micropore volume, but on the product of strong acidity and micropore volume. The selectivity to bulky di-branched isomers increased with micropore volume.

References

[1] R. Szostak, in: H. Van Bekkum, J.C. Flanigen, Jansen (Eds.), Introduction to Zeolite Science and Practice, 1991, pp. 153–192, Chapter 5, and reference therein.
[2] G.T. Kerr, J.N. Miale, R.J. Mikovsky, US Patent 3,493,519 (1970).
[3] R.M. Lago, W.O. Haag, R.J. Mikovsky, D.H. Oslon, S.D. Hellring, K.D. Schmitt, G.T. Kerr, in: Y. Murakami, A. Lijima, J.W. Ward (Eds.), Proceedings of the 7th Int. Zeolite Conf. Tokyo, Japan, August 17–22, Elsevier, Amsterdam, 1986, pp. 677–684.
[4] E. Loeffler, C.H. Peuker, H.G. Jerschkewitz, Catal. Today 3 (1988) 415.
[5] A. Hollo, Appl. Catal. 229 (2000) 93.
[6] A. Chica, Catal. Today 65 (2001) 101.
[7] H.W. Kouwenhoven, Molecular sieves ACS Advances in Chemistry Series, vol. 121, Am. Chem. Society, Washington, 1973, pp. 529.
[8] N. Essayem, Y. Ben Taarit, C. Feche, P.Y. Gayraud, G. Sapaly, C. Naccache, J. Catal. 219 (2003) 97.
[9] M.M. Olken, J.M. Garces, Proceedings of the 9th Int. Zeolite Conf., 1993, p. 559.
[10] G.R. Meima, M.J.M. Van der Aalst, M.S.U. Samson, J.M. Garces, G.J. Lee, Proceedings of the 9th Int. zeolite conference, 1993, p. 327.
[11] G.J. Lee, J.M. Garces, G.R. Meima, M.J.M. Van der Aalst, US Patent 32,517 (1989).
[12] J. Dwyer, Stud. Surf. Sci. Catal. 37 (1987) 765.
[13] F.N. Lin, E.D. Davis, US patent 6,140,547 (2000).
[14] J.A. Rabo, G.J. Gajda, in: D. Barthomeuf, E.G. Derouance, W. Hoelderich (Eds.), Guidelines for Mastering the Properties of Molecular Sieve, NATO ASI Series, B, Physics, 221, Plenum Press, New York, 1990, p. 273.
[15] G.R. Meima, CATTECH 2 (1998) 5.
[16] F. Raatz, C. Marcill, E. Freund, Zeolites 5 (1985) 5329.
[17] F. Raatz, C. Marcill, E. Freund, J. Chem. Soc. Farady Trans. 79 (1) (1983) 2299.
[18] J. Nagano, T. Eguchi, T. Asanuma, M. Nakayama, N. Nakamura, E.G. Derouane, Micropor. Mesopor. Mater. 33 (1999) 249.
[19] S. van Donk, A. Broersma, O.L.J. Gijzeman, J.A. van Bokhoven, J.H. Bitter, K.P. de Jong, J. Catal. 204 (2001) 272.

[20] B.L. Meyers, T.H. Fleisch, G.J. Ray, J.T. Miller, J.B. Hall, J. Catal. 110 (1998) 82.
[21] M.J.A. van Tromp, M.T. Garriga Oostenbrink, J.H. Bitter, K.P. de Jong, D.C. Koningsberger, J. Catal. 190 (2000) 209.
[22] F. Goovaerts, E.F. Vansant, J. Phillipaerts, P. De Hulsters, J. Gelan, J. Chem. Soc. Faraday Trans. I 85 (1989) 3675.
[23] N.S. Nesterenko, F. Thibault-Starzyk, V. Montouillout, V.V. Yuschenko, C. Fernandez, J.P. Gilson, F. Fajula, Ivanova II, Micropor. Mesopor. Mater. 71 (2004) 157.
[24] M. Guisnet, G. Perot, in: F. Ramoca Ribeiro, A.E. Rodringues, L.D. Rollmann, C. Naccache (Eds.), "Zeolites Science and Technology", NATO ASJ Series, The Hauge, 1984, pp. 397–420.
[25] M. Guisnet, V. Fouche, M. Bellon, J.P. Bournoville, C. Traves, Appl. Catal. 71 (1991) 283.
[26] Z.C. Shi, A. Auroux, Y. Ben Taarit, Can. J. Chem. 66 (1988) 1013.
[27] P.B. Koriada, J.R. Kiovsky, M.Y. Asim, J. Catal. 66 (1980) 290.
[28] L.O. Almanza, T. Narbeshuber, Appl. Catal. 178 (1999) 39–47.
[29] J.A. van Bokhoven, M. Tromp, D.C. Koningsberger, H.H. Kung, J. Catal. 202 (2001) 129–140.
[30] T.A.J. Hardenberg, L. Martens, P. Mesman, H.C. Muller, C.P. Nicolaides, Zeolites 12 (1992) 685.
[31] N. Viswanadham, M. Kumar, Micropor. Mesopor. Mater. 92 (2006) 31.
[32] T. Bucko, J. Hafner, L. Benco, J. Chem. Phys. 120 (2004) 10263.